Research Article

Shuai Sun*#, Jianxin Weng#, Yun Chen, Tingting Zheng, Yan Li, Jianfei Zhu, Yanjun Chen

LncRNA MIR17HG alleviates heart failure via targeting MIR17HG/miR-153-3p/SIRT1 axis in *in vitro* model

https://doi.org/10.1515/chem-2023-0146
received September 1, 2022; accepted October 9, 2023

Abstract: Heart failure (HF) is a syndrome of symptoms and signs caused by cardiac insufficiency and have become a serious global health problem. The aim of this study is to clarify the role and mechanism failure of MIR17HG. We established the *in vitro* HF model by using H_2O_2-treated AC-16 and HCM cells, and the reactive oxygen species (ROS) level and natriuretic peptide precursor B (NPPB) expression were also detected. The RNA expression of MIR17HG, miR-153-3p, SIRT1, and NPPB were detected by quantitative reverse transcription PCR while the SIRT1 and NPPB expression were detected by western blot. The binding relationship among MIR17HG, miR-153-3p, and SIRT1 were assessed by dual-luciferase reporter assay and RNA binding protein immunoprecipitation assay. Then, MIR17HG and SIRT1 were overexpressed by lentivirus transfection, and the influence of MIR17HG and SIRT1 on H_2O_2-induced apoptosis mediated by p53 were evaluated. The results show that MIR17HG and SIRT1 were significantly downregulated, while miR-153-3p was significantly upregulated in HF model. Overexpression of MIR17HG reduced miR-153-3p and alleviated HF, while knockdown of SIRT1 weakened the effects of MIR17HG, suggesting that SIRT1 was the direct target of MIR17HG/miR-153-3p axis. MIR17HG is significantly downregulated in HF model. Our research shows that MIR17HG protects cardiomyocytes from ROS-induced damage via the MIR17HG/miR-153-3p/SIRT1 axis, suggesting that MIR17HG and SIRT1 are potential therapeutic targets in HF.

Keywords: MIR17HG, miR-153-3p, SIRT1, heart failure, ROS, *in vitro* model

1 Introduction

Heart failure (HF) is a multifaceted clinical syndrome resulting from structural or functional defects in the heart, often the typical result of a variety of cardiovascular diseases [1]. HF pathologically leads to ventricular filling, diastolic dysfunction, and insufficient drainage of venous reflux, severely affecting human health. HF is often a result of conditions such as rheumatic heart disease, coronary heart disease, and hypertension [2]. HF currently exhibits high mortality and is associated with considerably poor prognosis. The increasing incidence rate of HF, largely due to an aging population, has escalated it to a significant global health issue [2,3]. Significant effort has been exerted toward the development of novel drugs against HF. Nonetheless, the 5 year survival of HF remains lower than that of human cancers [4]. The clinical diagnosis and treatment of HF present numerous challenges, necessitating effective health management.

The specific molecular mechanism behind how gene expression significantly influences the development of HF is yet to be fully identified [5]. The importance of pathways involving lncRNAs, miRNAs, and mRNAs in pathological conditions has been demonstrated [6,7]. lncRNAs are transcripts with lengths of at least 200 nucleotides. MicroRNAs, non-coding RNAs, post-transcriptionally modify the expression of target genes and impact numerous biological processes, contributing to the development of various human diseases through cell programming participation [8–10].

Sirtuins (SIRTs) represent a group of nicotinamide adenine dinucleotide (NAD)-dependent histone deacetylases, which are greatly preserved, and SIRT1 in particular has been the most extensively researched within the SIRTs family members [11]. Owing to their abundance in mammalian hearts, SIRT1 performs diverse functions in mediating

# Those authors have contributed equally in this work.

*** Corresponding author: Shuai Sun,** Department of Cardiology, Peking University Shenzhen Hospital, 1120 Lianhua Road, Shenzhen, Guangdong, 518000, P.R. China, e-mail: 358772811@qq.com, tel: +86-13924620363
Jianxin Weng, Yun Chen, Tingting Zheng, Yan Li, Jianfei Zhu, Yanjun Chen: Department of Cardiology, Peking University Shenzhen Hospital, Shenzhen, Guangdong, 518000, P.R. China

energetic metabolism in cardiomyocytes, producing reactive oxygen species (ROS), inducing angiogenesis, and inhibiting cardiomyocyte autophagy [12,13]. SIRT1 has been proved to protect the heart in HF by alleviating oxidative stress, fibrosis, and inflammatory response via the SIRT1/PCG-1α axis [14]. A prior investigation demonstrated a positive feedback loop connecting lncRNA MIR17HG and SIRT1 activity [15]. Despite this, scarcely any study about HF discusses the biological role of this feedback loop.

Apoptotic or necrotic cardiomyocytes cleared by the human body are replaced by newly formed scar tissues because cardiomyocytes are nonrenewable. As a result, inadequate blood circulation may lead to changes in the ventricle, ultimately resulting in HF [16]. Therefore, cardiomyocyte apoptosis is essential in the progression of HF. Two significant occurrences following HF are oxidative stress and the overproduction of ROS. In experimental analyses, H_2O_2 induction is a recognized method for establishing an *in vitro* or *in vivo* HF model [17,18]. In the present study, an *in vitro* HF model was established by H_2O_2 induction in AC-16 and HCM cells. We aim to clarify the regulatory effects of lncRNA MIR17HG and SIRT1 on the HF progression.

2 Methods and materials

2.1 Cell culture

The BeNa Culture Collection (BNCC) provided the human cardiomyocyte cell lines AC-16 and HCM (both from Bnbio in Beijing, China and listed under catalog numbers BNCC337712 and BNCC337719, respectively). The cells were cryopreserved at −80°C. The cultivation of these cells occurred in a humid environment composed of 5% CO_2 at 37°C, using Dulbecco's modified eagle medium (DMEM) mixed with 10% fetal bovine serum (FBS) and 1% penicillin-streptomycin. Trypsin was used to digest the cells into a singular cell suspension for transfer, a process that was continued until 80% confluence was achieved.

2.2 *In vitro* HF model

The cells experiencing logarithmic growth were broken down and re-suspended to reach a cell density of 1×10^4/mL. A volume of 2 mL of the cell suspension was then placed in each well of a six-well plate. Following a culture period of 24 h, the cells were subjected to 2.5% FBS in DMEM for 12 h in order to synchronize the cell cycle. After this, the control group's cells were grown in a fresh medium, while the experimental group's cells were grown in a medium that included 200 μM H_2O_2 [19]. After 6 h, relative levels of natriuretic peptide precursor B (NPPB) and ROS were examined to evaluate the success of the established *in vitro* HF model.

Table 1: Sequences of primers used in the experiment

Genes	Sequences
MIR17HG-F	5′-GGCGTCCCGTCGTAGTAAAG-3′
MIR17HG-R	5′-CATTGTGTCAGGAGTCAGTGTGTC-3′
miR-153-3p-F	5′-ACACTCCAGCTGGGTTGCATAGTCACAAA-3′
miR-153-3p-R	5′-CAGTGCGTGTCGTGGAGT-3′
SIRT1-F	5′-GTATTTATGCTCGCCTTGCTG-3′
SIRT1-R	5′-TGACAGAGAGATGGCTGGAA-3′
NPPB-F	5′-AAGGAGGCACTGGGAGAGGGGAAT-3′
NPPB-R	5′-CCCCACCAAGCCAACACAGGATGGA-3′
p53-F	5′-GAGCGAATCACGAGGGAC-3′
p53-R	5′-GCACAAACACGGACAGGA-3′
GAPDH-F	5′-AGCCACATCGCTCAGACAC-3′
GAPDH-R	5′-GCCCAATACGACCAAATCC-3′
U6-F	5′-CTCGCTTCGGCAGCACA-3′
U6-R	5′-AACGCTTCACGAATTTGCGT-3′

2.3 Quantitative reverse transcription PCR (RT-qPCR)

The RT-qPCR was used to check the mRNA levels of lncRNA MIR17HG, miR-153-3p, SIRT1, NPPB, and p53, utilizing GAPDH and U6 as internal references. The sequence of primers applied for RT-qPCR is given in Table 1. Using the TRIzol method, total RNAs were isolated from the cells and were later reverse transcribed into cDNAs after treating with the gDNA eraser using the Takara PrimeScriptTMRT reagent Kit. The RT-qPCR was then carried out for 40 cycles (95°C for 5 s, 60°C for 30 s, and 72°C for 40 s). The annealing process was eventually carried out for 10 min at 72°C. Each sample was detected in triplicate.

2.4 Western blot analysis

Through Western blot analysis, the protein levels of SIRT1, NPPB, p53, and acetylated p53 were assessed. The procedure involved an initial brief lysis of cells to extract cellular proteins. Subsequently, the protein concentration was measured using the bicinchoninic acid assay technique. Following denaturation, the protein samples were differentiated using gel electrophoresis at a rate of 50 μg per lane, and then applied to the polyvinylidene fluoride membranes. After being induced in TBST that contains 5% skim milk for 1 h, the membranes underwent immunoblotting. First, primary antibodies (diluted 1:1,000) were used at a temperature of 4°C overnight, followed by secondary antibodies (also diluted 1:1,000) at room temperature for an hour.

Enhanced chemiluminescence was then used to reveal the bands on the membrane, which were recorded for further analysis. Antibodies were purchased from Abclonal Biotech (Wuhan, China), the catalog numbers were listed as follows: SIRT1 (A19667), NPPB (A2179), p53 (A19585), acetylated p53 (A16324), and the secondary antibodies (AS014).

2.5 Determination of ROS level

AC-16 and HCM cells, post specific treatment, were cultured in a 24-well plate to 80% confluence and then incubated with 10 μmol/L DCFH-DA for half an hour at 37°C. Afterward, the fluorescence in five arbitrary fields in each well was recorded through a fluorescence microscope. Mean fluorescence intensity was computed, and the fluorescence density was quantified using ImageJ software. The calculation and normalization of the fluorescence density were carried out utilizing the Corrected Total Cell Fluorescence (CTCF) formula. The formula is defined as CTCF equals the integrated density subtracted by the product of the selected cell area and the average fluorescence from background readings.

2.6 Flow cytometry

Apoptosis in H_2O_2-treated cells for 6 h was measured using the apoptosis determination kit. After a digestion and resuspension process at a cellular density of 5×10^5/mL, the cells were stained with Annexin V-FITC in the absence of light. Flow cytometry (FACScan, BD Biosciences, Heidelberg, Germany) was used to identify apoptotic cells, which were successfully stained with Annexin V-FITC. The apoptosis rate is calculated by ($Q2 + Q3$).

2.7 Dual-luciferase reporter assay

The target relationship between MIR17HG and miR-153-3p, as well as that between miR-153-3p and SIRT1, was predicted using starBase and TargetScan and further assessed using the dual-luciferase reporter assay. Cobioer in Nanjing, China synthesized luciferase sequences that included both wild-type and mutant-type MIR17HG or SIRT13′-UTR. They were synthesized into DNAs following annealing and subjected to the construction of luciferase vectors alongside the pMiRGLO vector cleaved by restriction endonucleases NheI and SalI. After culturing with *Escherichia coli*, the corresponding plasmids were extracted, namely, pMiRGLO-MIR17HG-wt, pMiRGLO-MIR17HG-mut, pMiRGLO-SIRT1-3′-UTR-wt, and pMiRGLO-SIRT1-3′-UTR-mut. They were co-transfected into cardiomyocytes pre-cultured to 80% confluence in a 96-well plate either with miR-153-3p mimic or mimic-NC using Lipofectamine™ 2000. After 48 h, the cells were lysed in 100 μL of cell lysate per well and centrifuged at 12,000 rpm for 5 min. The supernatant, in a total volume of 50 μL, was gathered and directly combined with 100 μL of the Firefly luciferase detection reagent from Promega, Beijing, China. The mixture was then subjected to detection, with the results denoted in relative light units. Each group had three replicates.

2.8 RNA binding protein immunoprecipitation (RIP) assay

The RIP assay procedure, as detailed by Guo et al. [20], employed an EZ-Magna RIP Kit from Billerica, MA, USA. Cells achieved 80% confluence before AGO2-RIP experiments were initiated. The first step involved the use of RIP lysis buffer, containing proteinase and RNase inhibitors to lyse the cells. Afterward, the RIP lysates were exposed to RIP buffer, which incorporated magnetic beads coupled with either the human anti-Ago2 antibody or a nonspecific mouse IgG antibody provided by Millipore, Chicago, USA. Following this, the immunoprecipitate was digested using proteinase K, then processed through RT-PCR and gel-staining audits to ascertain MIR17HG enrichment. The RNA concentration was measured using a NanoDrop spectrophotometer. The cleaned RNA then went through a RT-qPCR analysis.

2.9 Cell transfection

RiboBio (Guangzhou, China) supplied MiR-153-3p mimic, mimic-NC, sh-SIRT1, and sh-NC. AC-16 and HCM cells were implanted in a 24-well plate and cultured to more than 70% confluence. They were subsequently cultivated in antibiotic-free DMEM for 4 h. Each well was supplemented with a concoction of transfection plasmids and polyethylenimine that was kept at room temperature for 40 min. After 24 h, it was substituted with a new medium imbued with 10% FBS and 1% penicillin-streptomycin. Transfection efficacy was ultimately assessed under a fluorescence microscope with FAM-labeled MiRNA as the control.

2.10 Lentiviral transfection

After cleaving the GV287 plasmid by using Age I, the sequence of MIR17HG was spliced, generating the overexpression plasmid of MIR17HG. The lentiviral packaging kit (GeneChem, Shanghai, China) was used to introduce the overexpression plasmid into 293T cells. The 293T cells

were cultivated to more than 80% confluence and then induced in Opti-MEM for 4 h. The Lenti-Easy Packaging Mix was mixed with the GV287-MIR17HG, or GV287 vector for 5 min at room temperature and subsequently mixed with Lipofectamine™ 2000 for 20 min. The transfection complex was used to transfect the 293T cells for a period of 3 days. Following this, the supernatant underwent collection and filtration in order to determine the viral titer. The AC-16 and HCM cells were cultivated to more than 80% confluence and then transfected with the corresponding lentivirus. The fluorescence intensity was observed on Days 3–4 to evaluate the efficiency of the lentivirus transfection.

2.11 Statistical processing

Data were expressed as mean value ± SD. Each experiment was conducted three times and analyzed using the one-tailed test in GraphPad Prism 8 software. A P value of less than 0.05 was deemed to be statistically significant.

3 Results

3.1 Establishment of the *in vitro* HF model

After cell culture for 24 h and synchronization of the cell cycle, human cardiomyocytes AC-16 and HCM were treated with 200 μM H_2O_2, to establish the *in vitro* HF model. The untreated control group had good cardiomyocyte growth, with a large number of cardiomyocytes, full cells, long cell protrusions, and adjacent cells interweave and grow in clusters, showing regular pulsation, low apoptosis rate, and extremely low NPPB expression level, which was the standard to judge the normal cardiomyocytes. Compared with those of negative controls, the mRNA levels of MIR17HG and SIRT1 were downregulated, whereas those of miR-153-3p and NPPB were upregulated in modeling cells (Figure 1a); consistent with this finding, the protein level of NPPB increased, whereas that of SIRT1 decreased following H_2O_2 treatment (Figure 1b). The ROS level was significantly increased in myocardial cells with oxidative damage (Figure1c), indicating the successful establishment of the *in vitro* HF model.

3.2 Confirmation of the binding interaction between lncRNA MIR17HG, miR-153-3p, and SIRT1

As predicted using starBase 2.0 (http://starbase.sysu.edu.cn/), a corresponding sequence was discovered within the MIR17HG and miR-153-3p sequences. Moreover, the complementary sequence located in the miR-153-3p and SIRT1 3′-UTR sequences was predicted using TargetScan 7.2

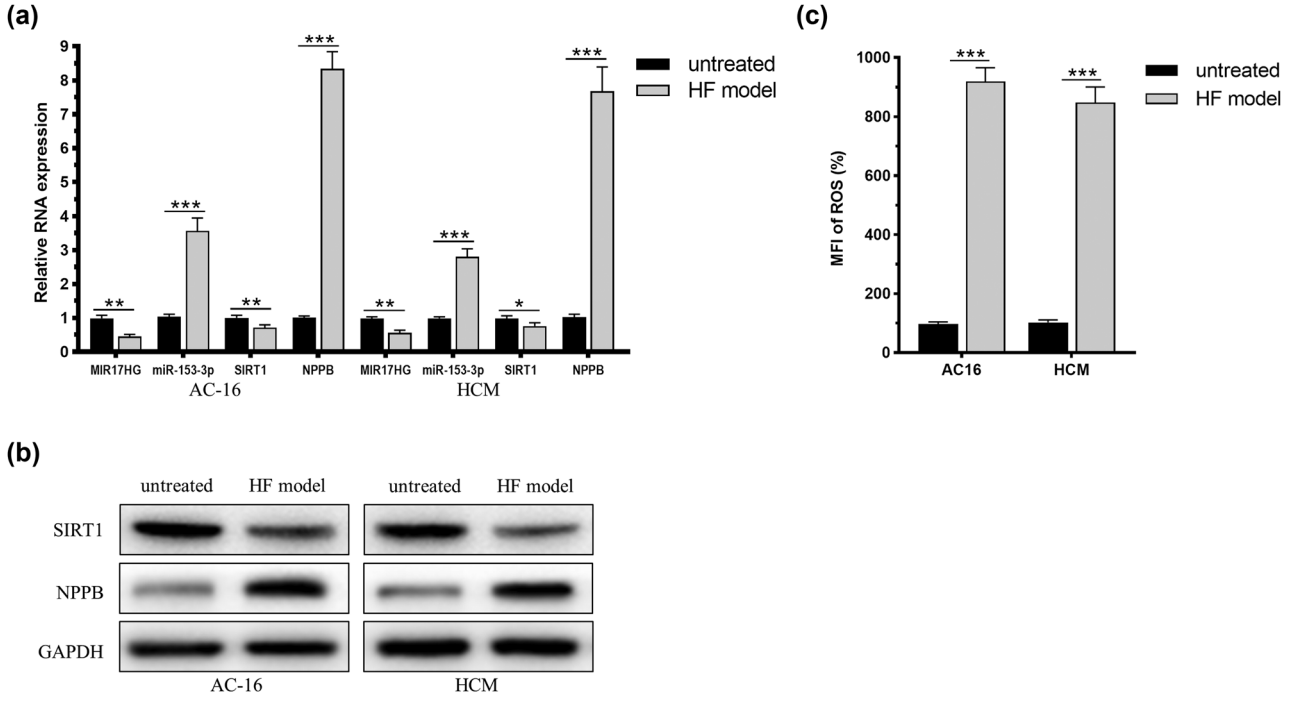

Figure 1: Establishment of the *in vitro* HF model. (a) Relative LncRNA MIR17HG, miR-153-3p and SIRT1 mRNA expression of AC-16 and HCM cell lines in HF model; (b) Relative SIRT1 and NPPB protein expression of AC-16 and HCM cell lines in HF model; (c) ROS level of AC-16 and HCM cell lines in HF model; (*P < 0.05; **0.001 ≤ P < 0.01; ***P < 0.001); MFI: Mean Fluorescence Intensity.

(http://www.targetscan.org/vert_72/) (Figure 2a). The dual-luciferase reporter assay determined that the luciferase intensity in cells co-transfected with pMiRGLO-MIR17HG-wt and miR-153-3p mimic was 41% of that of the blank group ($P < 0.05$). Moreover, when cells were co-transfected with pMiRGLO-SIRT1-3′-UTR-wt and miR-153-3p mimic, the intensity of the luciferase was 47% of that observed in the blank group, a statistically significant difference ($P < 0.05$). The luciferase intensity in the two control groups was 97 and 102% of those of the corresponding blank groups, respectively ($P > 0.05$). RIP assay also showed that lncRNA MIR17HG was associated with miR-153-3p (Figure 2c). The final inference confirmed the predicted sequence complementarities: MIR17HG has the ability to bind with miR-153-3p, which in turn can bind with SIRT1.

3.3 Ectopically expressed MIR17HG alleviates HF

Lentiviral transfection effectively upregulated MIR17HG in cardiomyocytes (Figure 3a). The relative level of ROS decreased in H_2O_2-treated cardiomyocytes overexpressing MIR17HG compared with the HF model groups (Figure 3b), and similar changes were observed in the apoptotic level (Figure 3c). Overexpression of MIR17HG in H_2O_2 – treated cardiomyocytes markedly downregulated miR-153-3p, NPPB, and p53 but upregulated SIRT1 (Figure 3d). Concurrently, there was a decrease in the protein levels of NPPB and acetylated p53 (acetyl-p53), but an increase in SIRT1 and p53 levels when compared to the HF model groups, as depicted in Figure 3e. The combined findings indicate that MIR17HG could protect cardiomyocytes from HF-induced injuries.

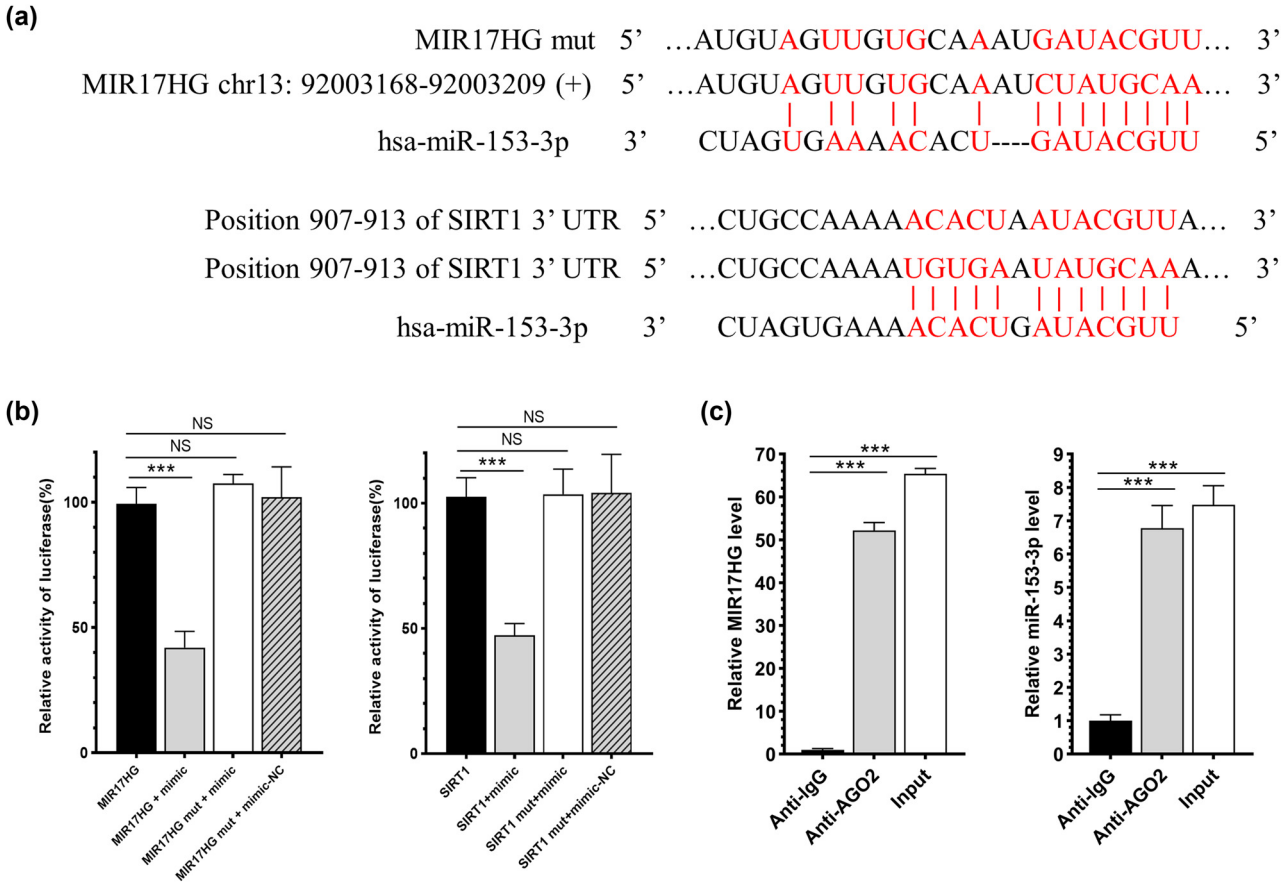

Figure 2: Confirmation of the binding interaction between lncRNA MIR17HG, miR-153-3p, and SIRT1. (a) Targeting relationship prediction based StarBase 3.0 and TargetScan 7.2; (b) relative activity of luciferase; (c) RIP assay showed that MIR17HG was associated with miR-153-3p; (*$P < 0.05$; **$0.001 \le P < 0.01$; ***$P < 0.001$).

3.4 MiR-153-3p reverses the regulatory effect of MIR17HG on HF

Overexpression of miR-153-3p in AC-16 and HCM cells was used to clarify the role of miR-153-3p in reversing the regulatory effect of MIR17HG on HF. The transfection with miR-153-3p mimic significantly increased the expression level of miR-153-3p, as shown in Figure 4a. Co-overexpression of miR-153-3p and MIR17HG and H_2O_2 treatment were subsequently conducted. Specifically, the overexpression of miR-153-p enhanced the ROS level (Figure 4b) and apoptotic rate (Figure 4c) in modeling cardiomyocytes. The combined overexpression of miR-153-3p and MIR17HG resulted in increased mRNA levels of NPPB and p53, yet it led to a decrease in SIRT1 compared to its overexpression with only MIR17HG (Figure 4d). Similarly, there was an elevation in the protein levels of NPPB and acetyl-p53, while levels of SIRT1 and p53 were reduced within cells co-overexpressing miR-153-3p and MIR17HG, as compared to cells singularly expressing MIR17HG (Figure 4e). The findings suggest that miR-153-3p could reverse the influence of MIR17HG on the biological behaviors of cardiomyocytes. MIR17HG mediated HF by targeting miR-153-3p.

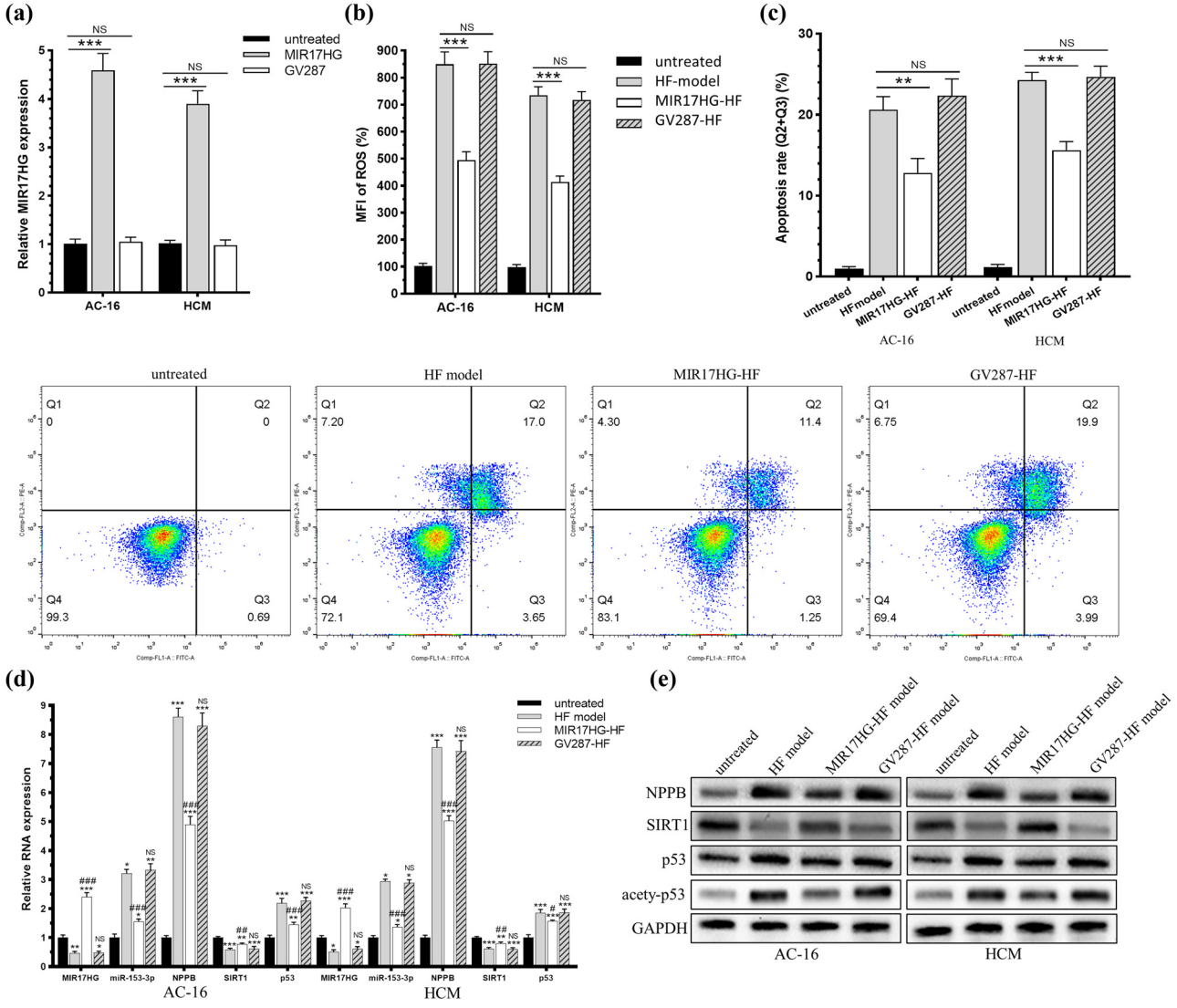

Figure 3: Ectopically expressed MIR17HG alleviates the progression of HF. (a) The efficiency of MIR17HG transfection; (b) elevating the expression of MIR17HG markedly lowered ROS levels in the HF model of AC-16 and HCM cells; (c) notably, the apoptosis rate of AC-16 and HCM cells in the HF model was significantly reduced by MIR17HG overexpression; (d) comparative RNA expression of AC-16 and HCM cells in the HF model; (e) comparison of protein levels in AC-16 and HCM cells in HF model; (*: vs untreated group; #: vs HF model group. */# $P < 0.05$; **/## $0.001 \le P < 0.01$; ***/### $P < 0.001$); MFI: Mean Fluorescence Intensity.

3.5 In mediating HF, miR-153-3p effectively targets SIRT1

The transfection efficacy of SIRT1 overexpressed in AC-16 and HCM cells was evaluated using RT-qPCR, as shown in Figure 5a. After H_2O_2 treatment in cardiomyocytes, the ROS level and apoptotic rate that were increased by the overexpression of miR-153-3p were also abolished by SIRT1 (Figure 5b and c). Simultaneously, overexpressed miR-153-3p markedly upregulated NPPB and acetyl-p53, which were effectively reversed by overexpressed SIRT1 (Figure 5d and e). The findings suggest that SIRT1 overexpression can efficiently suppress HF progression, with miR-153-3p capable of counteracting the SIRT1 effect. Thus, in the context of HF, SIRT1 is the miR-153-3p target.

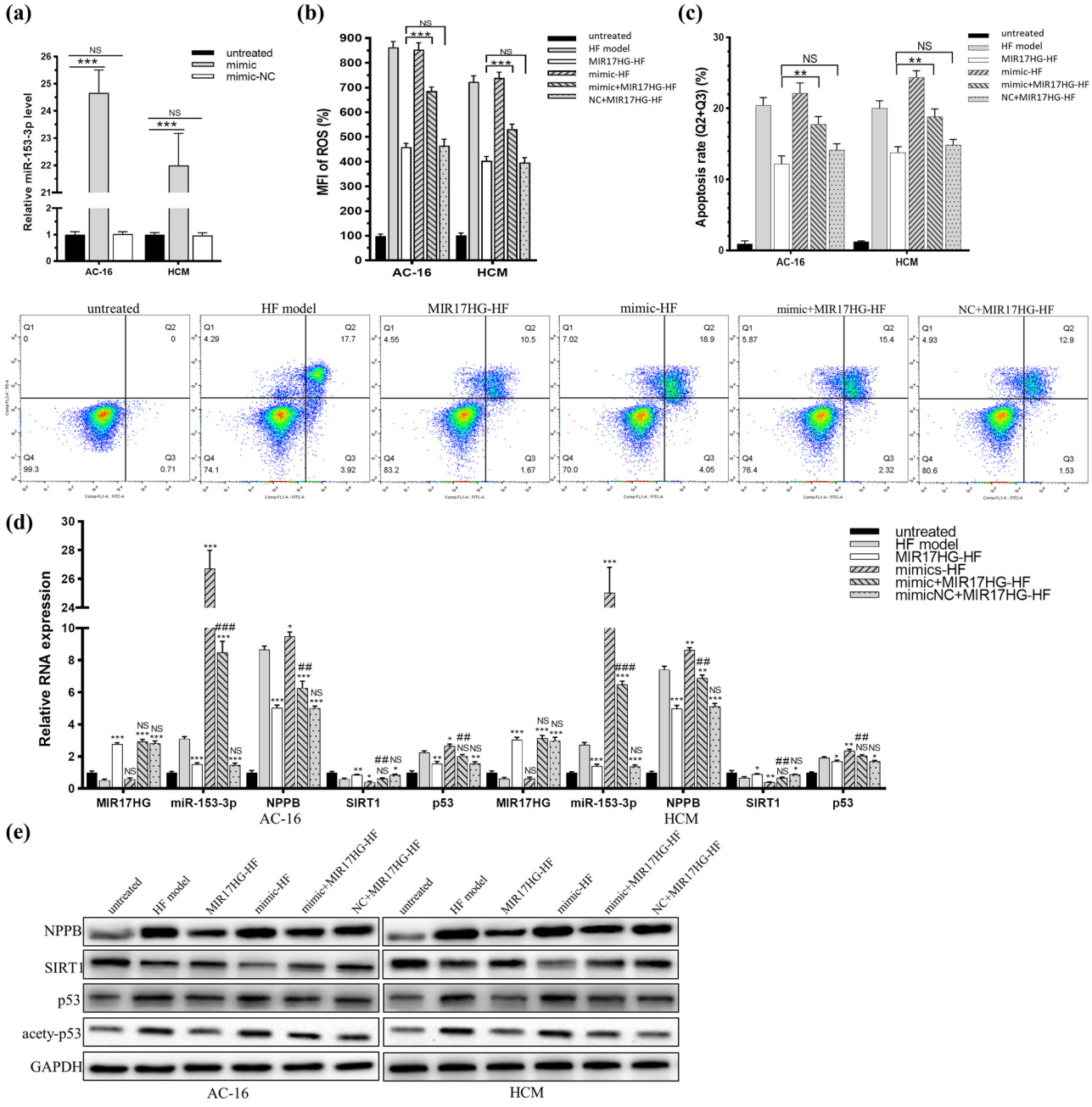

Figure 4: miR-153-3p reverses the regulatory effect of MIR17HG. (a) Transfection efficiency of miR-153-3p mimics; (b)–(e) overexpressed miR-153-3p could significantly reverse the effects of MIR17HG on AC-16 and HCM cells in HF model on (b) ROS level; (c) apoptosis rate of AC-16 and HCM cell lines; (d) relative RNA expression; (e) relative protein level; (*: vs HF model group; #: vs MIR17HG-HF group. */# $P < 0.05$; **/## $0.001 \le P < 0.01$; ***/### $P < 0.001$.); MFI: Mean Fluorescence Intensity.

3.6 LncRNA MIR17HG alleviates HF via the miR-153-3p/SIRT1 axis

The AC-16 and HCM cells were transfected with sh-SIRT1 or sh-NC, and the transfection efficacy was proven (Figure 6a). The cells transfected with sh-SIRT1 or sh-NC were further overexpressed by MIR17HG, followed by the establishment of the HF model. After SIRT1 knockdown, overexpressed MIR17HG no longer exerted a pronounced effect on neither ROS production (Figure 6b) nor apoptotic rate (Figure 6c). The results illustrated the substantial reversal of the effects of MIR17HG overexpression due to the knockdown of SIRT1. Conspicuously, there was a notable downregulation of miR-153-3p when MIR17HG was overexpressed.

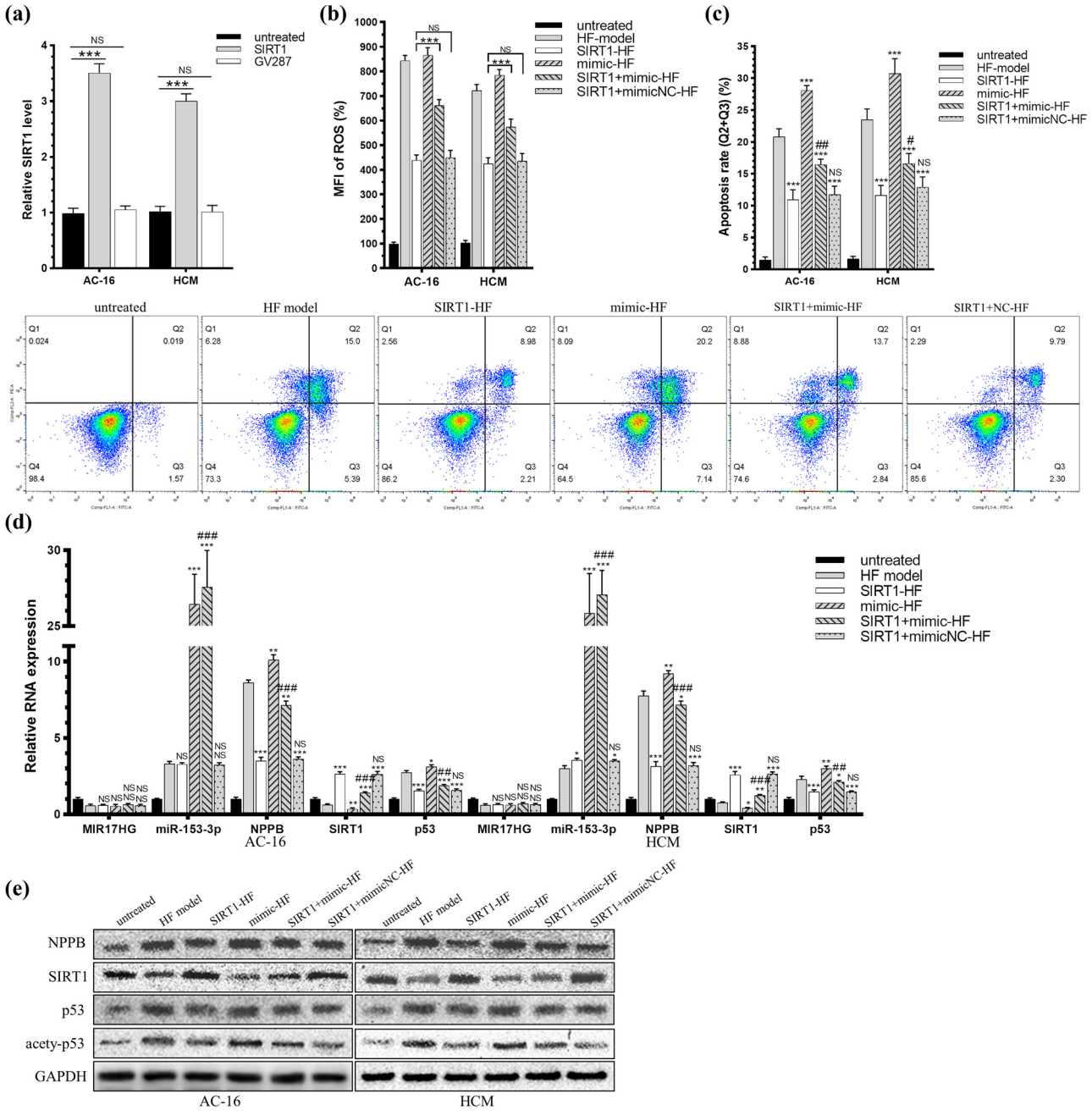

Figure 5: In mediating HF, miR-153-3p effectively targets SIRT1. (a) Transfection efficiency of lentivirus overexpressing SIRT1; (b)–(e) overexpressed SIRT1 could significantly reverse the effects of MiR-153-3p mimics on AC-16 and HCM cells in HF model on (b) ROS level; (c) apoptosis rate of AC-16 and HCM cell lines; (d) relative RNA expression; (e) relative protein level; (*: vs HF model group; #: vs SIRT1-HF group. */# $P < 0.05$; **/## $0.001 \le P < 0.01$; ***/### $P < 0.001$.); MFI: Mean Fluorescence Intensity.

However, the protein and mRNA levels of p53, acetyl-p53, and NPPB did not show any significant changes (Figure 6d and e). The above results suggested that SIRT1 is the final effector of MIR17HG in the HF model. Collectively, our results showed that MIR17HG alleviated HF via the miR-153-3p/SIRT1 axis.

4 Discussion

HF, is a syndrome pertaining to cardiac circulation that is provoked by both systolic and diastolic heart dysfunctions. It is often intensified by any structural or functional irregularities of the heart and represents the terminal phase of

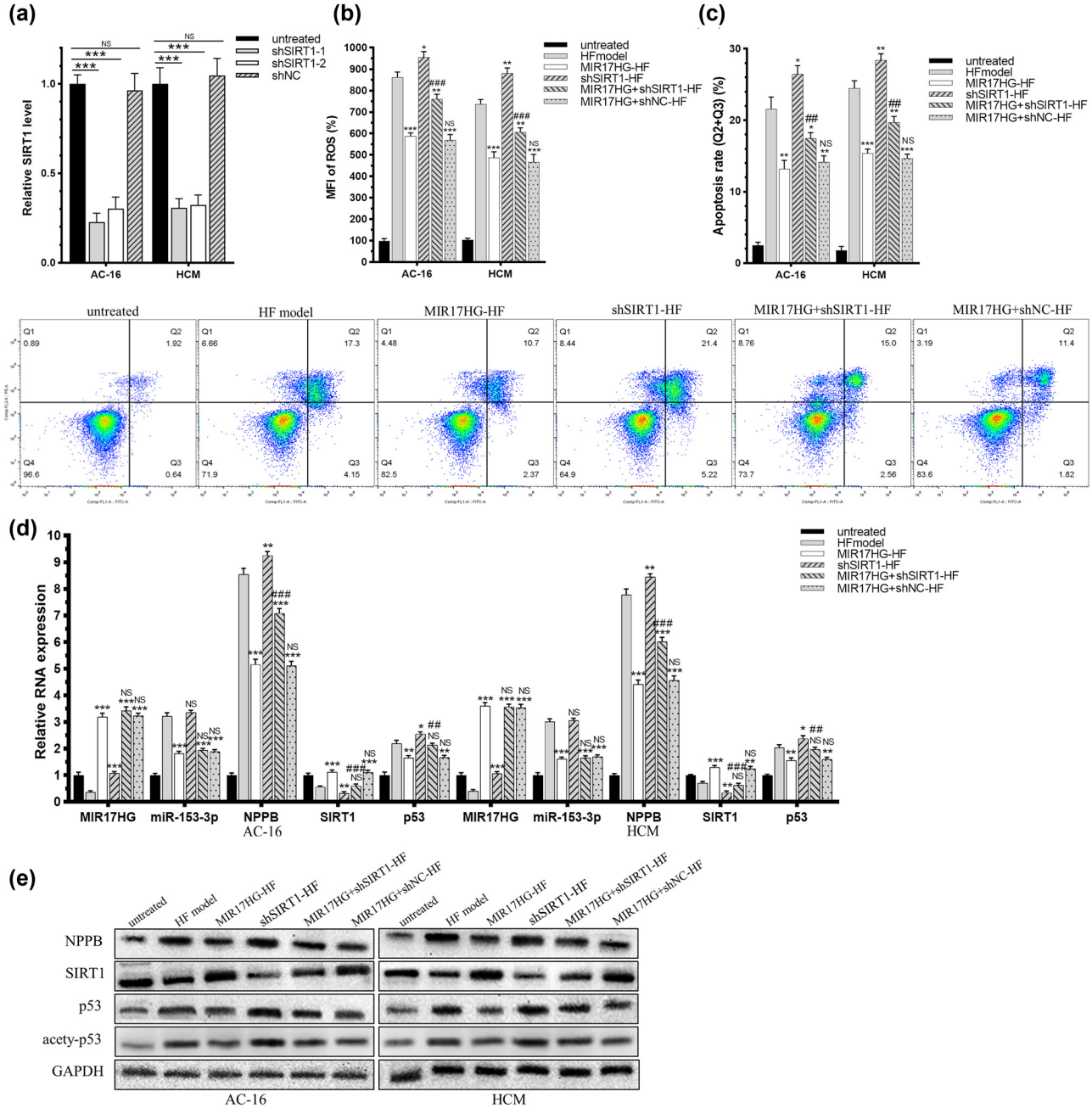

Figure 6: MIR17HG alleviates HF via the miR-153-3p/SIRT1 axis. (a) Transfection efficiency of sh-SIRT1; (b)–(e) Knocking down SIRT1 significantly inhibited the effects of MIR17HG on AC-16 and HCM cells in HF model on (b) ROS level; (c) apoptosis rate of AC-16 and HCM cell lines; (d) relative RNA expression; (e) relative protein level; (*: vs HF model group; #: vs MIR17HG-HF group. */# $P < 0.05$; **/## $0.001 \le P < 0.01$; ***/### $P < 0.001$.); MFI: Mean Fluorescence Intensity.

most cardiovascular conditions [1]. A variety of cardiovascular diseases, such as myocardial infarction (MI), hypertension, cardiomyopathy, and valvular heart disease, can contribute to the occurrence of HF [21]. Immediately after MI, the heart itself is remodeled such that it adjusts to a pathophysiological process involving the structural and functional alterations of cardiomyocytes, changes in the extracellular matrix of the non-infarcted myocardium, and so on. In the end, pathological heart lesions trigger notable alterations in the heart's form and capacity, continuous expansion of the ventricles, and pump failure, resulting in HF [22,23]. More precisely, crucial phenomena like immune activation, inflammatory response, oxidative stress, shifts in mitochondrial energy, and cell autophagy are all integral components of the HF process.

When the internal antioxidant defense system of a cell malfunctions, it can lead to a state called oxidative stress. This condition is characterized by the excessive buildup of oxygen-free radicals and related metabolites, which can harm the human body [24]. Oxidative stress can be understood as an imbalance between the body's innate ability to produce ROS and its potential antioxidant capacity [25]. An overproduction of ROS can result in cellular dysfunction, lipid and protein peroxidation, and damage to DNA. Consequently, cells are injured or die inevitably, providing the fundamental basis of cardiovascular diseases. Meanwhile, excessive accumulation of ROS triggers the activation of pro-inflammatory factors, with an inflammatory response as a sign [26]. H_2O_2 induction is commonly applied to establish an *in vivo* or *in vitro* HF model. Furukawa et al. [27] showed that H_2O_2 accelerates cellular senescence by accumulation of acetyl-p53 via decrease in the function of SIRT1 by NAD+ depletion. Zhang et al. [28] demonstrated that the inflammatory factor Mzb1 is a vital regulator of cardiomyocytes following MI, which markedly improves mitochondrial function and blocks inflammation signaling in H_2O_2-induced neonatal mice as a potential therapeutic target of ischemic cardiomyopathy. Wei et al. [18] established an *in vitro* HF model by H_2O_2 treatment in H9C2 rat cardiomyocytes. They proved that lncRNA NEAT1 stimulates the pathological process of HF by downregulating miR-129-5p. Consistent with these findings, the current study successfully established HF models in AC-16 and HCM cells, which were verified by detecting relative levels of NPPB and ROS.

LncRNAs comprise the most major type of non-coding RNAs. They contain no open reading frame and are scarce and exhibit relatively poor primary sequence conservation. It is important to note that lncRNAs exhibit characteristics that are specific to the tissue, cell, and stage, and these particular features are intimately connected with pathological processes [29,30]. LncRNAs generally perform their biological functions by binding to ribonucleoproteins. A growing volume of evidence has revealed that the regulatory effects of lncRNAs rely on the lncRNA–miRNA–target gene axis. Moreover, some lncRNAs can bind to DNAs and recruit chromatin-modifying proteins, forming RNA–DNA–protein complexes and thereby mediating downstream genes [31]. While potential mechanisms may differ among various disease types or cells, the contribution of lncRNAs to the progression of cardiovascular diseases has been recognized [32]. Thus, lncRNAs have drawn interest and have been widely discussed related to cardiovascular diseases. Wu et al. [33] reported that when MI occurs, p53 is activated in hypoxia-induced cardiomyocytes, further upregulating MEG3. Zhang et al. [34] detected relative levels of MHRT in the plasma of HF patients and evaluated its diagnostic potential for chronic HF by ROC curve analysis. They revealed that the overexpression of MHRT reduces H_2O_2-induced apoptosis AC-16 cells.

The host gene of several miRNAs, LncRNA MIR17HG, is linked with cell death and the level of its expression is related to cell apoptosis. Recently, the focus of various studies has been the biological role of MIR17HG in cancer. Wei et al. [35] showed that MIR17HG is downregulated in non-small-cell lung cancer cases, which inhibits the invasive and migratory capacities of cancer cells by upregulating miR-142-3p via methylation modification and thus downregulates Bach-1. Nonetheless, the involvement of MIR17HG in cardiovascular diseases is rarely reported. A case of a 14-year-old boy experiencing aortic stenosis, short stature, hearing loss, and minor learning disabilities was discussed in the report by Grote et al. [36]. The study employed microarray-based comparative genomic hybridization to discover a roughly 3.6 Mb interstitial heterozygous deletion at 13q31.3, including MIR17HG. This finding hints at a potential link between MIR17HG and cardiovascular diseases. In this study, MIR17HG acts as a molecular sponge to directly target miR-153-3p, and miR-153-3p can target downstream factors to regulate cell apoptosis. Zou et al. [37] showed that miR-153 regulated apoptosis and autophagy by targeting Mcl-1, that regulated cardiomyocyte survival during oxidative stress. Our study found that MIR17HG was downregulated in HF model, while the rate of myocardial cell apoptosis after overexpression of MIR17HG induced by hydrogen peroxide was lower than that of the control group. Further functional experiments showed that miR-153-3p can upregulate the acetylation of SIRT1 and p53. It is possible for MIR17HG to competitively bind with miR-153-3p in order to manage the acetylation of SIRT1 and p53, hinder apoptosis of cardiomyocytes triggered by ROS, and therefore mitigate the advancement of HF.

SIRT1 is a class of histone deacetylases, and its influence on protein deacetylation is an important posttranslational modification process. SIRT1 is highly expressed in the heart of mammals, which is responsible for mediating cardiomyocyte metabolism, ROS production, angiogenesis, and autophagy. SIRT1 also participates in the process of HF [38]. Xie et al. established an *in vivo* HF rat model by Adriamycin induction. Their results showed that administering kallistatin to HF rat models alleviates inflammatory response and cell apoptosis in the rat myocardium by upregulating SIRT1, which protects HF-induced myocardium injury [39]. Hariharan et al. [40] and Gottlieb et al. [41] showed that SIRT1 could activate Rab7 by deacetylating FOXO1. Consequently, the autophagy of starvation-induced cardiomyocytes is mediated, damaged mitochondria are eliminated, and apoptosis is blocked, thus rescuing a dying myocardium. SIRT1 is reported to eliminate mitochondrial ROS by enhancing MnSOD activity via HIF-2α, which relieves symptoms such as decreased cardiac ejection fraction, myocardial fibrosis, and myocardial necrosis [42]. The results of our study showed that knockdown of SIRT1 in cardiomyocytes attenuated the effects of both MiR-153-3p and MIR7HG on the HF model. miR-153-3p was demonstrated to bind to SIRT1 3′-UTR, and SIRT1 was proved to be the specific target of miR-153-3p. The aforementioned data indicated that SIRT1 is the direct target of MIR17HG and miR-153-3p, which were implicated in HF.

5 Conclusion

Through the MIR17HG/miR-153-3p/SIRT1 axis, the lncRNA MIR17HG safeguards cardiomyocytes from damage induced by ROS. This implies that MIR17HG could be a promising therapeutic target for HF.

Funding information: Shenzhen Science and Technology Innovation Committee (JCYJ20180302173917265, KCXFZ20-20020110104874), Basic Research Special Project of Shenzhen (Natural Science Foundation) (2021300357).

Author contributions: S.S. and Y.C.: methodology, investigation, project administration, writing – original draft, data curation, and funding acquisition. J.W. and T.Z.: formal analysis, investigation, data curation, visualization, formal analysis, validation, investigation, resources, investigation. Y.L., J.Z., and Y.C.: data curation, visualization, conceptualization, writing – review and editing.

Conflict of interest: The authors declare no conflicts of interest related to this study.

Ethical approval: The conducted research is not related to either human or animal use.

Data availability statement: The datasets generated during and/or analyzed during the current study are available from the corresponding author on reasonable request.

Reference

[1] Luscher TF. Heart failure: the cardiovascular epidemic of the 21st century. Eur Heart J. 2015;36(7):395–7.
[2] Li X, Liao J, Jiang Z, Liu X, Chen S, He X, et al. A concise review of recent advances in anti-heart failure targets and its small molecules inhibitors in recent years. Eur J Med Chem. 2020;186:111852.
[3] Ambrosy AP, Fonarow GC, Butler J, Chioncel O, Greene SJ, Vaduganathan M, et al. The global health and economic burden of hospitalizations for heart failure: lessons learned from hospitalized heart failure registries. J Am Coll Cardiol. 2014;63(12):1123–33.
[4] Braunwald E. The war against heart failure: the Lancet lecture. Lancet. 2015;385(9970):812–24.
[5] Yang J, Xu WW, Hu SJ. Heart failure: advanced development in genetics and epigenetics. BioMed Res Int. 2015;2015:352734.
[6] Wang JY, Yang Y, Ma Y, Wang F, Xue A, Zhu J, et al. Potential regulatory role of lncRNA-miRNA-mRNA axis in osteosarcoma. Biomed Pharmacother. 2020;121:109627.
[7] Zhang R, Jiang YY, Xiao K, Huang XQ, Wang J, Chen SY. Candidate lncRNA-miRNA-mRNA network in predicting hepatocarcinogenesis with cirrhosis: an integrated bioinformatics analysis. J Cancer Res Clin Oncol. 2020;146(1):87–96.
[8] Cuevas-Diaz Duran R, Wei H, Kim DH, Wu JQ. Invited Review: Long non-coding RNAs: important regulators in the development, function and disorders of the central nervous system. Neuropathol Appl Neurobiol. 2019;45(6):538–56.
[9] Nie L, Zhang P, Wang Q, Zhou X, Wang Q. lncRNA-triggered macrophage inflammaging deteriorates age-related diseases. Mediators Inflamm. 2019;2019:4260309.
[10] Cui M, Liu Y, Cheng L, Li T, Deng Y, Liu D. Research progress on anti-ovarian cancer mechanism of miRNA regulating tumor microenvironment. Front Immunol. 2022;13:1050917.
[11] Mimura T, Kaji Y, Noma H, Funatsu H, Okamoto S. The role of SIRT1 in ocular aging. Exp Eye Res. 2013;116:17–26.
[12] D'Onofrio N, Servillo L, Balestrieri ML. SIRT1 and SIRT6 signaling pathways in cardiovascular disease protection. Antioxid Redox Signal. 2018;28(8):711–32.
[13] Alcendor RR, Gao S, Zhai P, Zablocki D, Holle E, Yu X, et al. SIRT1 regulates aging and resistance to oxidative stress in the heart. Circ Res. 2007;100(10):1512–21.
[14] Waldman M, Cohen K, Yadin D, Nudelman V, Gorfil D, Laniado-Schwartzman M, et al. Regulation of diabetic cardiomyopathy by caloric restriction is mediated by intracellular signaling pathways involving 'SIRT1 and PGC-1alpha'. Cardiovasc Diabetol. 2018;17(1):111.
[15] Xie L, Huang R, Liu S, Wu W, Su A, Li R, et al. A positive feedback loop of SIRT1 and miR17HG promotes the repair of DNA double-stranded breaks. Cell Cycle. 2019;18(17):2110–23.
[16] Minicucci MF, Azevedo PS, Polegato BF, Paiva SA, Zornoff LA. Heart failure after myocardial infarction: clinical implications and treatment. Clin Cardiol. 2011;34(7):410–4.

[17] Zhang L, Wang YN, Ju JM, Shabanova A, Li Y, Fang RN, et al. Mzb1 protects against myocardial infarction injury in mice via modulating mitochondrial function and alleviating inflammation. Acta Pharmacol Sin. 2020;42(5):691–700
[18] Wei Q, Zhou HY, Shi XD, Cao HY, Qin L. Long noncoding RNA NEAT1 promotes myocardiocyte apoptosis and suppresses proliferation through regulation of miR-129-5p. J Cardiovasc Pharmacol. 2019;74(6):535–41.
[19] Martinez J, Perez-Serrano J, Bernadina WE, Rodriguez-Caabeiro F. Oxidative and cold shock cause enhanced induction of a 50 kDa stress protein in Trichinella spiralis. Parasitol Res. 2002;88(5):427–30.
[20] Guo W, Huang J, Lei P, Guo L, Li X. LncRNA SNHG1 promoted HGC-27 cell growth and migration via the miR-140/ADAM10 axis. Int J Biol Macromol. 2019;122:817–23.
[21] Tsutsui H, Tsuchihashi-Makaya M, Kinugawa S, Goto D, Takeshita A, Investigators J-G. Characteristics and outcomes of patients with heart failure in general practices and hospitals. Circ J Off J Jap Circ Soc. 2007;71(4):449–54.
[22] Gajarsa JJ, Kloner RA. Left ventricular remodeling in the post-infarction heart: a review of cellular, molecular mechanisms, and therapeutic modalities. Heart Fail Rev. 2011;16(1):13–21.
[23] Pfeffer JM, Pfeffer MA, Fletcher PJ, Braunwald E. Progressive ventricular remodeling in rat with myocardial infarction. Am J Physiol. 1991;260(5 Pt 2):H1406–14.
[24] Reuter S, Gupta SC, Chaturvedi MM, Aggarwal BB. Oxidative stress, inflammation, and cancer: how are they linked? Free Radic Biol Med. 2010;49(11):1603–16.
[25] Willcox JK, Ash SL, Catignani GL. Antioxidants and prevention of chronic disease. Crit Rev Food Sci Nutr. 2004;44(4):275–95.
[26] Hussain T, Tan B, Yin Y, Blachier F, Tossou MC, Rahu N. Oxidative stress and inflammation: What polyphenols can do for us? Oxid Med Cell Longev. 2016;2016:7432797.
[27] Furukawa A, Tada-Oikawa S, Kawanishi S, Oikawa S. H_2O_2 accelerates cellular senescence by accumulation of acetylated p53 via decrease in the function of SIRT1 by NAD + depletion. Cell Physiol Biochem. 2007;20(1–4):45–54.
[28] Zhang L, Wang YN, Ju JM, Shabanova A, Li Y, Fang RN, et al. Mzb1 protects against myocardial infarction injury in mice via modulating mitochondrial function and alleviating inflammation. Acta Pharmacol Sin. 2021;42(5):691–700.
[29] Quinn JJ, Chang HY. Unique features of long non-coding RNA biogenesis and function. Nat Rev Genet. 2016;17(1):47–62.
[30] Gupta SC, Awasthee N, Rai V, Chava S, Gunda V, Challagundla KB. Long non-coding RNAs and nuclear factor-kappaB crosstalk in cancer and other human diseases. Biochim et Biophys Acta Rev Cancer. 2020;1873(1):188316.
[31] Quinodoz S, Guttman M. Long noncoding RNAs: an emerging link between gene regulation and nuclear organization. Trends Cell Biol. 2014;24(11):651–63.
[32] Lozano-Vidal N, Bink DI, Boon RA. Long noncoding RNA in cardiac aging and disease. J Mol Cell Biol. 2019;11(10):860–7.
[33] Wu H, Zhao ZA, Liu J, Hao K, Yu Y, Han X, et al. Long noncoding RNA Meg3 regulates cardiomyocyte apoptosis in myocardial infarction. Gene Ther. 2018;25(8):511–23.
[34] Zhang L, Wu YJ, Zhang SL. Circulating lncRNA MHRT predicts survival of patients with chronic heart failure. J Geriatric Cardiol: JGC. 2019;16(11):818–21.
[35] Wei S, Liu J, Li X, Liu X. LncRNA MIR17HG inhibits non-small cell lung cancer by upregulating miR-142-3p to downregulate Bach-1. BMC Pulm Med. 2020;20(1):78.
[36] Grote LE, Repnikova EA, Amudhavalli SM. Expanding the phenotype of feingold syndrome-2. Am J Med Genet Part A. 2015;167A (12):3219–25.
[37] Yuhau Z, Wenting L, Jinxia Z, Dingcheng X. miR-153 regulates apoptosis and autophagy of cardiomyocytes by targeting Mcl-1. Mol Med Rep. 2016;14(1):1033–9.
[38] Hsu CP, Odewale I, Alcendor RR, Sadoshima J. SIRT1 protects the heart from aging and stress. Biol Chem. 2008;389(3):221–31.
[39] Xie J, Yu QG, Yang LL, Sun YY. Kallistatin alleviates heart failure in rats by inhibiting myocardial inflammation and apoptosis via regulating SIRT1. Eur Rev Med Pharmacol Sci. 2020;24(11):6390–9.
[40] Hariharan N, Maejima Y, Nakae J, Paik J, Depinho RA, Sadoshima J. Deacetylation of FOXO by SIRT1 plays an essential role in mediating starvation-induced autophagy in cardiac myocytes. Circ Res. 2010;107(12):1470–82.
[41] Gottlieb RA, Finley KD, Mentzer RM. Cardioprotection requires taking out the trash. Basic Res Cardiol. 2009;104(2):169–80.
[42] Sano M, Minamino T, Toko H, Miyauchi H, Orimo M, Qin Y, et al. p53-induced inhibition of HIF-1 causes cardiac dysfunction during pressure overload. Nature. 2007;446(7134):444–8.